

Large Amplitude Undulations on the Equatorward Boundary of the Diffuse Aurora

A. T. Y. LUI, C.-I. MENG, AND S. ISMAIL

Applied Physics Laboratory, The Johns Hopkins University, Laurel, Maryland 20707

Global auroral pictures from the Defense Meteorological Satellite Program (DMSP) satellites are presented to show, for the first time, occurrences of large amplitude undulations on the equatorward boundary of the diffuse aurora in the afternoon-evening sector. The crest-to-trough amplitude of these waveforms ranges from about 40 to 400 km and the wavelength varies from about 200 to 900 km. The undulations are seen in one case to extend over 3000 km along the equatorward boundary. Auroral images from successive DMSP passes suggest that this phenomenon lasts for about 0.5 to 3.5 hours. In each of the four cases observed, the undulations occur during a geomagnetic storm interval near the peak development of the storm time ring current. In all instances, auroral pictures displaying the undulations show simultaneous substorm patterns of discrete auroras. In one instance when simultaneous electron (50 eV to 20 keV) measurements from DMSP satellite are available, the electron spectra near the diffuse auroral equatorward boundary resemble power law spectra, and the scale length for the density gradient at the boundary is determined to be about 12 km. Weak electron precipitation is also found equatorward of the diffuse aurora and the associated electron spectra frequently show a secondary population with peak fluxes at 1–5 keV. The observed undulations are interpreted as surface waves propagating on the inner edge of the plasma sheet, and possible plasma instabilities responsible for it are briefly discussed.

INTRODUCTION

Morphological studies of global auroral distributions have led to many descriptive terms of aurora. Among them are the mantle aurora [Sandford, 1968], the continuous aurora [Whalen *et al.*, 1971; Buchau *et al.*, 1972], and the diffuse aurora [Lui and Anger, 1973]. These three different terms originate from different observational techniques of some widespread auroral emissions in the auroral region. Whereas the correspondence between the mantle aurora and the diffuse aurora is still unsettled [Lui *et al.*, 1973, 1975b; Anger *et al.*, 1974; Shepherd *et al.*, 1976], there is a general consensus that the continuous aurora and the diffuse aurora refer to the same type of auroral particle precipitation [Pike and Whalen, 1974; Akasofu, 1974a, b; Snyder *et al.*, 1974; Lui *et al.*, 1975a; Whalen *et al.*, 1977].

The diffuse (or continuous) aurora equatorward of the discrete auroral region in the auroral oval represents the optical 'foot print' of the low latitude or central plasma sheet [Lui *et al.*, 1973, 1977; Winningham *et al.*, 1975; Meng *et al.*, 1979; Burke *et al.*, 1980]. Its luminosity is enhanced during substorm disturbances [Lui *et al.*, 1973, 1975a; Murphree and Anger, 1978] and also is reported to vary periodically (2 to 40 s period) for both quiescent and pulsating forms of the diffuse aurora [Berkey, 1980]. Pulsating auroras are identified within the diffuse auroral region [Siren, 1975, 1978; Royovik and Davis, 1977; Davis *et al.*, 1978]. It has been proposed that the mechanisms for the precipitation of diffuse auroral particles (electrons and protons) are a field-aligned current driven instability at low altitudes and an ion loss cone instability at large radial distances [Ashour-Abdalla and Thorne, 1978]. A current convective instability is also suggested to be operative in the diffuse aurora to produce ionospheric *F* region irregularities [Ossakow and Chaturvedi, 1979].

The equatorward boundary of the diffuse aurora has been widely used in characterizing the size of the auroral oval and in monitoring the magnetospheric configurational response to the interplanetary magnetic field and substorm activity [Lui *et al.*, 1975a; Kamide and Winningham, 1977; Sheehan and Carovillano, 1978; Slater *et al.*, 1980; Gussenhoven *et al.*, 1981]. In addition, the equatorward boundary has been treated as a convenient reference boundary for tracing source locations of ground-based or low-altitude phenomena into the magnetosphere. For instance, the magnetospheric location for the plasma injection boundary [Eather *et al.*, 1976; Sheehan and Carovillano, 1978] and the substorm initiation region [Lui and Burrows, 1978] with respect to the inner edge of the plasma sheet have been inferred in this manner.

The equatorward boundary of the diffuse aurora is usually seen by satellite auroral imaging systems to be a smooth boundary, i.e., there is no drastic latitudinal variation or waveform as a function of magnetic local time. In this paper, we report the first observation of large scale undulations in the equatorward boundary of the diffuse aurora by pictures of global auroral displays in the afternoon-evening sector. These observations are made by a broad band scanning radiometer on the Defense Meteorological Satellite Program (DMSP) satellites [Rogers *et al.*, 1974; Pike and Whalen, 1974; Pike, 1974; Pike and Gardner, 1981].

UNDULATIONS ON THE EQUATORWARD DIFFUSE AURORAL BOUNDARY

We discuss four periods during which the equatorward boundary of the diffuse aurora is undulated. Three of these are taken in the southern polar region and one in the northern polar region. The auroral images from DMSP satellites are all shown in negative. Each auroral picture is composed of successive scanning strips nearly perpendicular to the satellite subtrack, yielding one picture per pass over the polar region. The scan width is about 3000 km on the ground and about 2500 km at 100-km altitude (see, e.g., Pike and Gardner [1981]).

Copyright © 1982 by the American Geophysical Union.

Paper number 1A1751.
0148-0227/82/001A-1751\$05.00



Fig. 1a. Undulation on the equatorward boundary of the diffuse aurora in the afternoon-evening sector seen by DMSP/F1 satellite on June 26, 1978 at about 2141 UT in the southern hemisphere.

June 26, 1978

A spectacular display of undulations on the equatorward boundary of the diffuse aurora is shown in Figure 1a. The DMSP satellite (F1) crosses the southern auroral oval at about 2141 UT on June 26, 1978 and views the afternoon-evening sector. The undulations on the equatorward boundary of the diffuse aurora, resembling ripples on a water surface, are seen

over a distance of about 3000 km. At least seven complete wave cycles can be identified. The amplitude of the undulations increases from evening to afternoon local time for five cycles, indicating either a growth of the wave as it approaches the afternoon hours or a damping of the wave as it moves toward the evening local times.

The observed undulations are unlikely to be a result of temporal variations of auroral intensity such as in pulsating

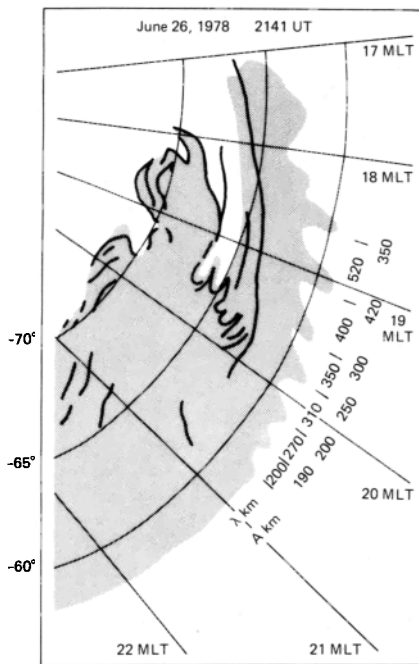


Fig. 1b. A sketch of the main auroral features seen at about 2141 UT on June 26, 1978 with a superposition of an approximate grid of magnetic latitudes and magnetic local time. The approximate wavelength λ and crest-to-trough amplitude A for each wave cycle are shown adjacent to the waveform.

auroras. According to *Siren* [1975], pulsating auroras detected in DMSP pictures have a zebra-stripe appearance, which is quite distinct from the ripple patterns reported here. In addition, the continuous contour of the wave pattern across many adjacent scanning strips and sometimes abrupt variations at three locations within one single scanning strip would require extremely artificial and irregular matching of the temporal intensity fluctuations with the scanning frequency.

Accompanying this phenomenon is a large surge pattern of discrete auroras along the poleward portion of the auroral oval. This westward traveling surge pattern suggests that a substorm is progressing at this time. Figure 1b is a sketch of some main auroral features seen. Unfortunately, the fiducial information for this pass is not available on the log sheet. However, an approximate grid for magnetic latitudes and magnetic local times can be overlaid. It is also possible to estimate the approximate wavelength λ (distance for a complete cycle) and the crest-to-trough amplitude A since they do not require the information of the precise geographic location given by the log sheet. It can be determined that the wavelength varies from 200 to 520 km and the crest-to-trough amplitude ranges from 190 to 420 km. The wavelength increases monotonically toward the earlier local time. Similar monotonic increases in amplitude can be noted until the waveform at ~ 1900 MLT, where the amplitude starts to decrease from 420 km to 350 km.

Another point worthy of addressing is this. Since, in most cases, it is difficult to calibrate the sensitivity of the DMSP images in terms of absolute auroral intensity, there remains a possibility that the undulations noted here may lie within a weak diffuse aurora demarcated by a smooth equatorward boundary. This is considered rather unlikely, however, because a close examination of the intensities around the

undulations in Figure 1a reveals a steep luminosity gradient associated with the undulated waveform. Judging from this gradient, it may be estimated that the undulations would be apparent for the range of threshold intensities from ~ 0.5 to ~ 5 kR (in 3914 Å) and that the shape of the contour of the equatorward boundary is relatively independent of the sensitivity threshold. Furthermore, the sharp gradient in auroral intensity is consistent with the usual signature of the equatorward boundary of the diffuse aurora [Lui and Anger, 1973; Lui et al., 1975a; Kamide and Winningham, 1977; Sheehan and Carovillano, 1978].

At about 2240 UT, approximately 1 hour later, another DMSP satellite (F3) passes over the same area in the evening sector of the southern auroral oval. Figure 2a shows the auroral image obtained at that time. The equatorward boundary of the diffuse aurora is still noticeably undulated, although the extension of these waveforms to the left-hand side of the picture is obscured by sunlight interference. Three cycles of waveforms can be recognized. The low latitude extrusions of the boundary in these waveforms tend to bend toward the midnight, resembling a wave steepening pattern. Similar to the previous pass by F1 satellite, a large surge-type auroral pattern is seen at the poleward portion of the auroral oval. Figure 2b is a sketch of the main auroral features. It indicates that the approximate wavelength changes from 440 km in one cycle to 640 km in the next. The crest-to-trough amplitude varies from 220 to 300 km. The increase in wavelength and amplitude toward earlier magnetic local time is similar to that seen in Figures 1a and 1b between 1900 and 2100 MLT.

Figure 3a shows the auroral image obtained during the pass of DMSP satellite F3 over the southern polar region at about 2058 UT. This pass precedes the one for Figure 2a. The wavelike modulation of the equatorward boundary of the diffuse aurora is still distinguishable but with a much smaller amplitude; as more clearly indicated in Figure 3b. There is an arc-like luminosity feature equatorward of the diffuse aurora. This may possibly be the detached arcs (and patches) phenomenon that has been observed by the ISIS 2 auroral imaging system [Moshupi, 1977; Moshupi et al., 1977; Anger et al., 1978; Moshupi et al., 1979; Wallis et al., 1979].

There are low-energy electron detectors onboard the DMSP satellites [Hardy et al., 1979]. Unfortunately, particle data for the above three passes are not available. Therefore, the precipitating electron characteristics along the undulated equatorward boundary of the diffuse aurora for these events cannot be determined.

July 4, 1978

Figure 4a shows the auroral morphology in the southern polar region viewed by the DMSP satellite (F2) at about 1609 UT. The strikingly unusual auroral phenomenon is the large-scale deformation of the equatorward boundary of the diffuse aurora, similar to the previous events. Spacings between the peaks or the low-latitude extrusions of the diffuse aurora are, however, quite irregular in this case. The peak-to-crest amplitudes range from 40 to 240 km. A faint arclike luminosity is also visible equatorward of the diffuse aurora near the later evening hours, between 1700 and 1800 MLT. This feature resembles the detached arcs reported by the ISIS 2 group [e.g., Moshupi et al., 1979]. At the poleward portion of the auroral



Fig. 2a. Auroral picture from the DMSP/F3 satellite that shows the global auroral display in the same area as in Figure 1a but about 1 hour later; i.e., at about 2240 UT on June 26, 1978.

oval, a small auroral surge pattern is seen, indicating again that the large-scale undulation of the equatorward diffuse auroral boundary occurs within a substorm interval. Some of the main auroral features are sketched in Figure 4b, together with a superposition of magnetic latitudes and magnetic local times. It may be noted that the undulation extends over

1500–1800 MLT in the evening sector, at latitudes $\sim -61^\circ$. This low-latitude diffuse auroral boundary suggests that it is an expanded auroral oval and the geomagnetic activity is high [Lui *et al.*, 1975a; Kamide and Winningham, 1977; Sheehan and Carovillano, 1978; Slater *et al.*, 1980].

There are low-energy electron measurements from the same

DMSP satellite for this pass. Figure 5a shows the profiles of the number flux (top trace), the energy flux (middle trace), and the average energy (bottom trace) of precipitating electrons in the energy range of ~ 50 eV to 20 keV along the satellite track. The energy coverage is made in 16 energy bins from 2 curved-plate electrostatic analyzers [Huber *et al.*, 1977; Hardy *et al.*, 1979]. The count rates across the entire polar region from 3 representative channels (0.26, 2.3, 20 keV) are provided in Figure 5b. The satellite crosses the equatorward boundary of the diffuse aurora in the interval of 1610:25 to 1610:45 UT. Selected electron spectra across the diffuse auroral boundary are provided in Figure 6a. It can be seen that the spectra resemble power law rather than Maxwellian spectra. In addition, we have found traces of energetic electron precipitation equatorward of the diffuse aurora at latitudes about -59.7 to -60.3 . The particle spectra frequently show a prominent secondary population with some similarity to those associated with discrete auroras. The peak flux occurs in the energy range of 1–5 keV. Some representative spectra are plotted in Figure 6b. This precipitation probably corresponds to the auroral feature seen equatorward of the diffuse aurora. Wallis *et al.* [1979] reported seeing a similar secondary peak at somewhat higher energies (5–6 keV) in electron spectra associated with detached arcs and patches.

In order to determine the scale lengths for the gradients across the equatorward diffuse auroral boundary, the number density per unit solid angle $dN/d\Omega$ and energy density per unit solid angle $dW/d\Omega$ across the boundary are evaluated numerically from the observed fluxes $j(E)$ by

$$\begin{aligned} \frac{dN}{d\Omega} &= \int_{E_{min}}^{E_{max}} j(E) \sqrt{\frac{m_e}{2E}} dE \\ &\approx \sum_{i=2}^{15} j(E_i) \sqrt{\frac{m_e}{2E_i}} \frac{E_{i+1} - E_{i-1}}{2} \end{aligned}$$

and

$$\begin{aligned} \frac{dW}{d\Omega} &= \int_{E_{min}}^{E_{max}} j(E) \sqrt{\frac{m_e E}{2}} dE \\ &\approx \sum_{i=2}^{15} j(E_i) \sqrt{\frac{m_e E_i}{2}} \frac{E_{i+1} - E_{i-1}}{2} \end{aligned}$$

where m_e is the electron mass, E_i and $j(E_i)$ are, respectively, the center energy and observed differential flux of the i th channel. The computed results are shown in Figure 7. At latitudes below the diffuse aurora where very weak precipitation is detected (1610:20–1610:26 UT), $dN/d\Omega \sim 0.015$ $\text{cm}^{-3}\text{sr}^{-1}$ and $dW/d\Omega \sim 4 \times 10^{-3}$ $\text{keV cm}^{-3}\text{sr}^{-1}$. After the equatorward boundary is crossed ($\sim 1610:42$ UT) $dN/d\Omega \sim 0.4$ $\text{cm}^{-3}\text{sr}^{-1}$ and $dW/d\Omega \sim 6 \times 10^{-2}$ $\text{keV cm}^{-3}\text{sr}^{-1}$. The magnetic latitudes of the spacecraft at 1610:26 UT and 1610:42 UT are -60.4° and -60.8° . The increases in number density and energy density across the equatorward boundary are about a factor of 27 and 15, respectively. Therefore the scale length for the number density gradient at the equatorward boundary of the diffuse aurora is ~ 12 km and that for the energy density gradient is ~ 14 km. There are two large 1-s enhancements of electron fluxes at 1610:33 and 1610:40 UT. Since this is the only case in which particle measurements are available across the undulated boundary, it

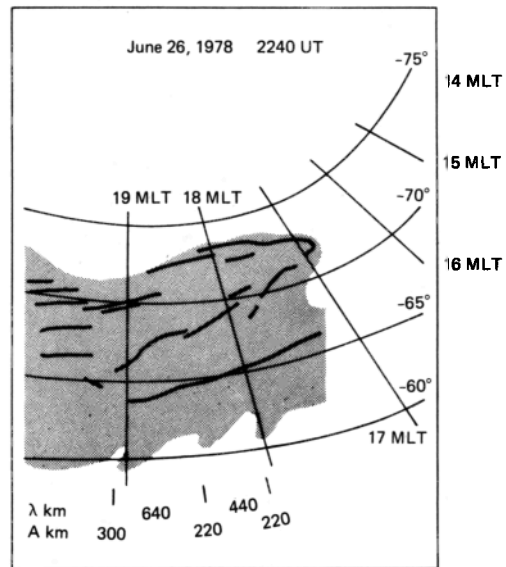


Fig. 2b. A sketch of the main auroral features seen in Figure 2a with an overlay of magnetic latitudes and magnetic local time.

is uncertain at the present time whether or not these enhancements are significant in the occurrence of undulations reported here. Future studies may clarify this.

One further comment on this pass is necessary. When the magnetic latitude and magnetic local time grid is overlaid on the basis of the fiducial information available from the log sheet, it is found that the resulting latitude for the equatorward diffuse auroral boundary is considerably lower ($\sim 3^\circ$) than that provided with particle measurements at the time of the equatorward crossing of the diffuse auroral precipitation. However, if we assume the fiducial time is inadvertently taken from the adjacent fiducial mark on the DMSP picture, good agreement is found on the latitudes of both the equatorward and poleward boundaries of the auroral precipitation between the particle data and auroral picture. Therefore, we believe that the fiducial time is inadvertently misread and entered in the log sheet, and the grid overlay based on our interpretation is given in Figure 4b.

July 8, 1975

Figures 8a and 8b show another unusual occurrence of 'ripples' on the equatorward boundary of the diffuse aurora at ~ 1148 UT in the southern auroral oval. At least five cycles of waveforms can be identified with wavelengths in the range of ~ 260 to 340 km and with the crest-to-trough amplitudes from ~ 110 to 240 km. The wavelength and amplitude are the smallest at MLT closest to the midnight within the coverage of the imaging system. Both parameters increase from ~ 1900 MLT to ~ 1800 MLT where they appear to decrease further on. A small surge pattern is seen at the poleward portion of the diffuse aurora. Unfortunately, no low-energy electron data are available for this satellite pass.

January 25, 1979

The extrusions seen at the equatorward boundary of the diffuse aurora can sometimes be extremely irregular. This is



Fig. 3a. Auroral image from DMSP/F3 satellite at about 2058 UT on June 26, 1978.

indicated in Figures 9a and 9b by the DMSP image obtained during a northern polar region pass at about 0406 UT. The shape of the equatorward boundary does not suggest any simple waveform. The largest extrusion or amplitude in this case is ~ 340 km. The discrete auroral pattern in the poleward portion of the auroral oval resembles a portion of a large surge or auroral bulge near the peak phase of a substorm.

DURATION OF THE UNDULATIONS

The duration of the observed undulations on the equatorward boundary of the diffuse aurora is investigated by examining DMSP passes preceding and subsequent to those presented in the previous section.

For the occurrences on June 26, 1978, no undulation is seen

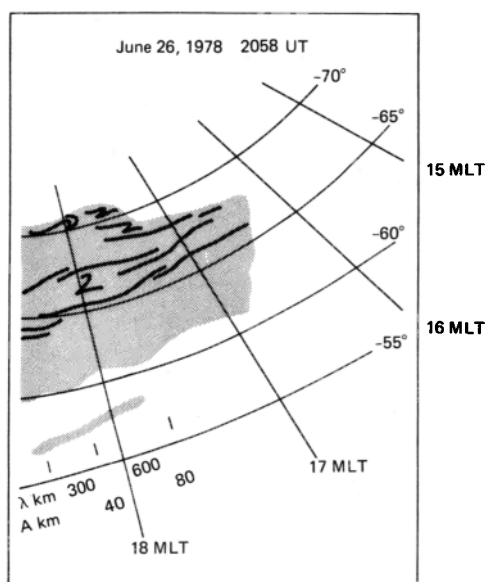


Fig. 3b. A sketch of the main auroral features in Figure 3a.

for the DMSP/F1 pass at about 1944 UT and for the DMSP/F2 pass at about 2317 UT. This indicates that the undulations are present for more than 2 hours (from about 2058 UT to 2240 UT; Figures 1a–3a) but less than 3.5 hours.

For the event on July 4, 1978, the undulations are not observed at about 1359 UT by the DMSP/F1. They are, however, seen at about 1445 UT by DMSP/F3. At about 1540 UT, the DMSP/F1 passes over the southern auroral oval again. The auroral oval has expanded considerably at this time, with the result that the equatorward boundary of the diffuse aurora extends outside the imager's field of view. It is, therefore, uncertain whether or not the undulations still exist. On the subsequent pass of DMSP/F1 at about 1722 UT, the undulations are not seen. This information indicates that the undulations last for at least 1.5 hours (from about 1445 UT to 1609 UT) but not longer than 3.5 hours.

For the July 8, 1975, case, it is found that there is a slight indication of undulations on the equatorward boundary of the diffuse aurora from DMSP/F1 observation as early as at about 0303 UT, which later develop to a marked low-latitude extrusion of the diffuse aurora at about 0342 UT seen by DMSP/31. Undulations on the equatorward boundary are then seen at about 0445 UT when the DMSP/F1 passes over the southern auroral oval. However, at 0523 UT the undulations seem to disappear based on DMSP/31 observation at that time. Some indication of undulations later reappears at about 0951 UT although the identification is hindered by the sunlit portion of the auroral picture. This unfavorable viewing condition is also found for the pass at about 1315 UT. Judging from these observations, it appears that the undulations may have occurred in two intervals, from about 0303 UT to 0445 UT and from about 0951 UT to 1315 UT. The duration in this case is again between 1.5 and 3.5 hours.

For the fourth case on January 25, 1979, there is no indication of undulations at about 0209 UT as seen by DMSP/F3. Marginal indication of undulations is observed at about 0342 UT by DMSP/F1 and at 0349 UT by DMSP/F2. The undulations seem to have gone at 0524 UT based on the DMSP/F1 auroral picture. In other words, the undulations in

this case appear to occur at least between 0342 UT and 0406 UT, a duration of about 0.5 hour.

From these four instances, it appears that the undulations on the equatorward boundary of the diffuse aurora usually last about 0.5 to 3.5 hours. The occurrence of the observed undulations is very uncommon, however. This can be recognized from the fact that DMSP pictures are available to the science community since 1972 and this is the first report of this auroral phenomenon. A concrete number on its occurrence frequency will be determined in future statistical studies.

GEOMAGNETIC AND INTERPLANETARY CONDITIONS

The rather unusual occurrence of undulations at the equatorward boundary of the diffuse aurora is found to be closely tied to intense geomagnetic activity. Of the four days in which this phenomenon is found, two of them, July 8, 1975, and July 4, 1978, are the most disturbed days of the month. The other two are the second most disturbed days of the month. The Kp index, the daily sum Kp , and the Dst values for the periods of interest are given in Table 1 under the heading of geomagnetic conditions. The large negative values of Dst suggest that the intervals concerned are during the progress of geomagnetic storms. A plot of Dst values in Figure 10a indeed shows the development of the geomagnetic storms corresponding to these events. The event of July 8, 1975, occurs about 7 hours after the peak of a storm with a maximum Dst of -67 nT. Similarly, the event of June 26, 1978, occurs about 5 hours after the storm peak with a maximum Dst of -98 nT. For the July 4, 1978, event, the time coincides with a brief large negative excursion of -114 nT in the Dst index. This is almost the same value as the Dst index at the peak of the geomagnetic storm 14 hours later (maximum $Dst \sim -113$ nT). The fourth event on January 25, 1979 is associated with the second of two successive geomagnetic storms. The time of the event precedes the peak of the second storm (maximum $Dst \sim -58$ nT) by about 7 hours.

The available AE index during the events is given in Figure 10b. For July 8, 1975, the AE index is obtained from Allen *et al.* [1980]. The undulation on the equatorward diffuse auroral boundary are seen in the early recovery phase of a substorm in which the peak disturbance reaches about 1200 nT. The 'AE index' for June 26, 1978, and July 4, 1978, is constructed from the American International Magnetospheric Study (IMS) magnetic station network listed in Table 2. A substorm with peak disturbance of ~ 2000 nT occurs near the time of the event on July 4, 1978, when the Dst index shows a large negative excursion. For the event on June 26, 1978, the 'AE index' shows only a moderate value of about 500 nT. However, this may be due to the poor station coverage at that particular UT interval.

The information on the interplanetary conditions during which the undulations are seen at the equatorward boundary is less complete. Under the heading of interplanetary conditions in Table 1, the parameters given are the solar wind speed V_{sw} (km/s), number density n (cm^{-3}), temperature (10^3 K), interplanetary magnetic field magnitude B (nT), and the magnetic field components in solar magnetospheric coordinates B_x , B_y , B_z (nT) [King, 1979]. All these parameters are known only for the event on July 8, 1975. In



Fig. 4a. Another occurrence of undulation on the equatorward diffuse auroral boundary seen by DMSP/F2 satellite at about 1609 UT on July 4, 1978.

this case, the solar wind speed and the temperature are somewhat normal. Only the number density and the magnetic field, especially the southward component, are rather large. On the basis of polar cap magnetograms [*Lincoln, 1975, 1978a,b*], the interplanetary sector boundary occurs within one day of the occurrence of this phenomenon (there is un-

certainty on the sector boundary crossing for the January 25, 1979, event).

SUMMARY

We have presented four intervals during which large-scale undulations on the equatorward boundary of the diffuse

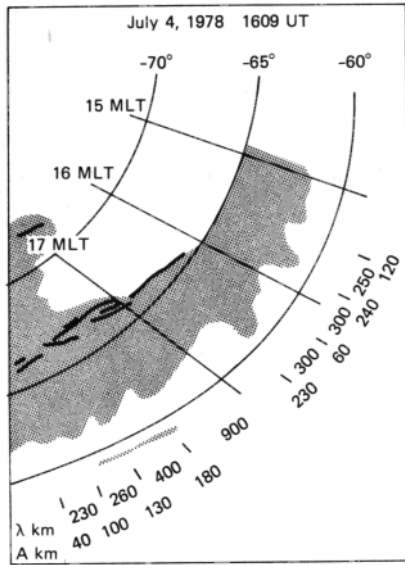


Fig. 4b. Some of the main auroral features seen in Figure 4a are schematically illustrated.

aurora are seen. The approximate wavelength ranges from ~ 200 to 900 km, and the approximate crest-to-trough amplitude varies from about 40 to 420 km. Several features are noted:

1. In all cases the undulations are seen in the evening-afternoon local time sector.
2. All occur during the period of a geomagnetic storm near the peak development of the storm-time ring current.
3. All are accompanied by substorm patterns of discrete

auroras, i.e., westward traveling surge or auroral bulge.

4. In three cases, the wave amplitude and wavelength generally first show an increase towards earlier local times and then a decrease. Owing to the limited local time coverage, it is uncertain whether the fourth case also shows such a trend.

5. Undulations appear to have durations of about 0.5 to 3.5 hours.

6. The electron spectra in the energy range of 50 eV to 20 keV resemble power laws rather than Maxwellian spectra near the equatorward boundary of the diffuse aurora. However, weak precipitation with electron spectra showing a prominent secondary population are seen equatorward of the diffuse aurora.

7. The scale length for the electron density gradient at the equatorward boundary is about 12 km.

While the first five features can be considered as common to all events, the last two features that are determined for only one case may or may not be common. It may be worthwhile to mention that other cases of undulation at a smaller scale, although not shown here, can be found in the DMSP/F2 auroral images, e.g., January 26, 1979, ~ 0331 UT, orbit 8502. Therefore, the lower limit on the amplitude is somewhat arbitrary.

DISCUSSION

Even though DMSP images essentially provide 'snapshots' of the undulations on the equatorward boundary of the diffuse aurora, it is important to assess the temporal behavior of the undulations. The fact that these undulations may endure for a few hours raises the possibility that this boundary deformation may be rather stationary or non-propagating. However, although the information provided by

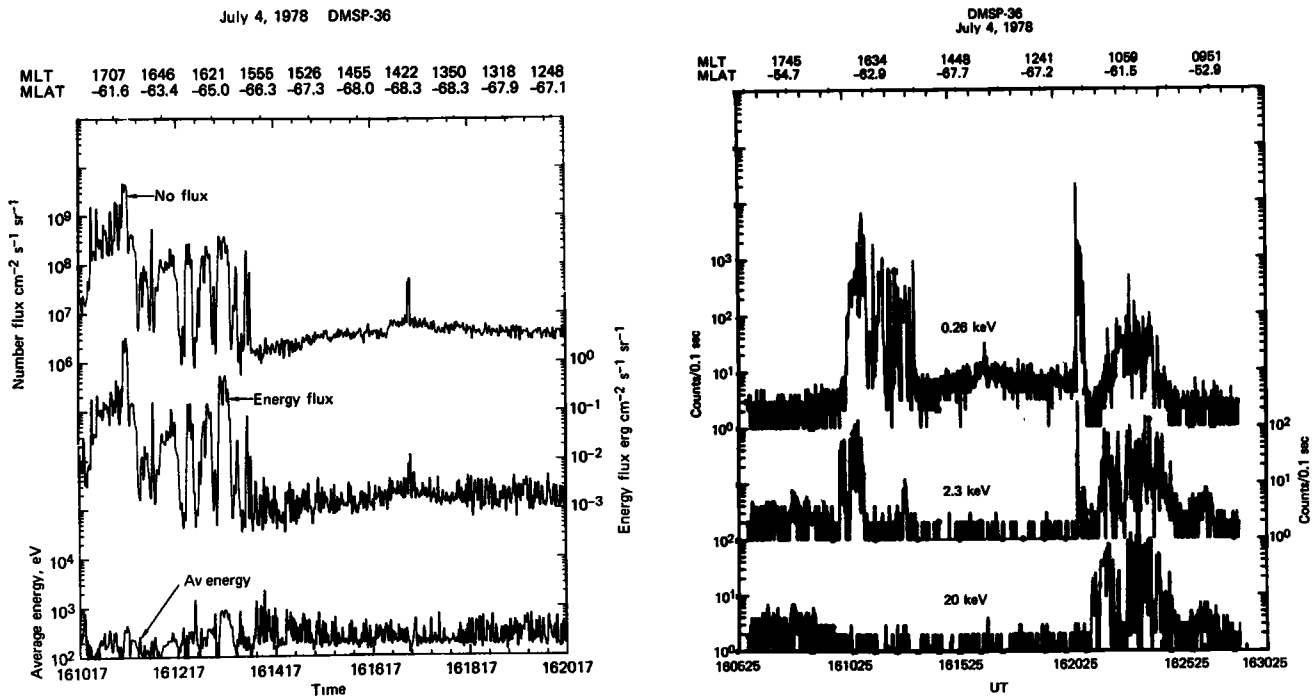


Fig. 5. (a) The latitudinal profiles of number flux, energy flux, and averaged energy of precipitating electrons measured by the electron detector on DMSP/F2 during the same pass as that for Figure 4a. (b) Latitudinal profiles of count rates from 3 representative channels at 0.26, 2.3, and 20 keV.

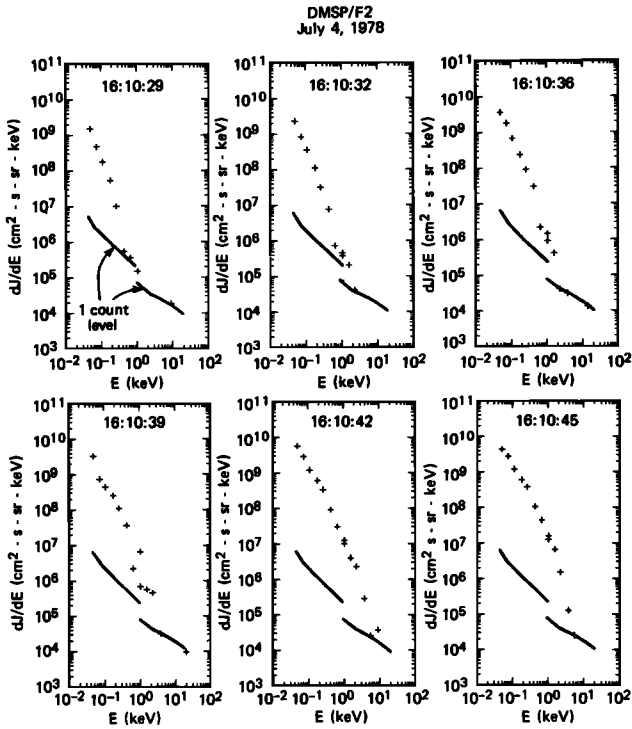


Fig. 6a. Spectra of precipitating electrons across the diffuse auroral boundary on July 4, 1978. The time of the measurement is shown in each panel. The one-count levels in the two detectors are indicated by the solid lines.

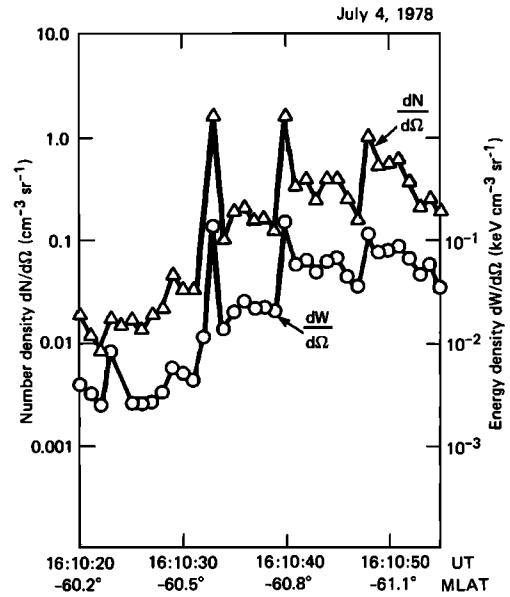


Fig. 7. Computed number density $dN/d\Omega$ and energy density $dW/d\Omega$ across the diffuse auroral boundary.

the snapshots is rather limited, we may consider this to be rather unlikely for the reason that in Figures 1b, 2b, and 4b, the waveforms show low-latitude crests bending toward midnight. These features suggest that the phase velocity of the

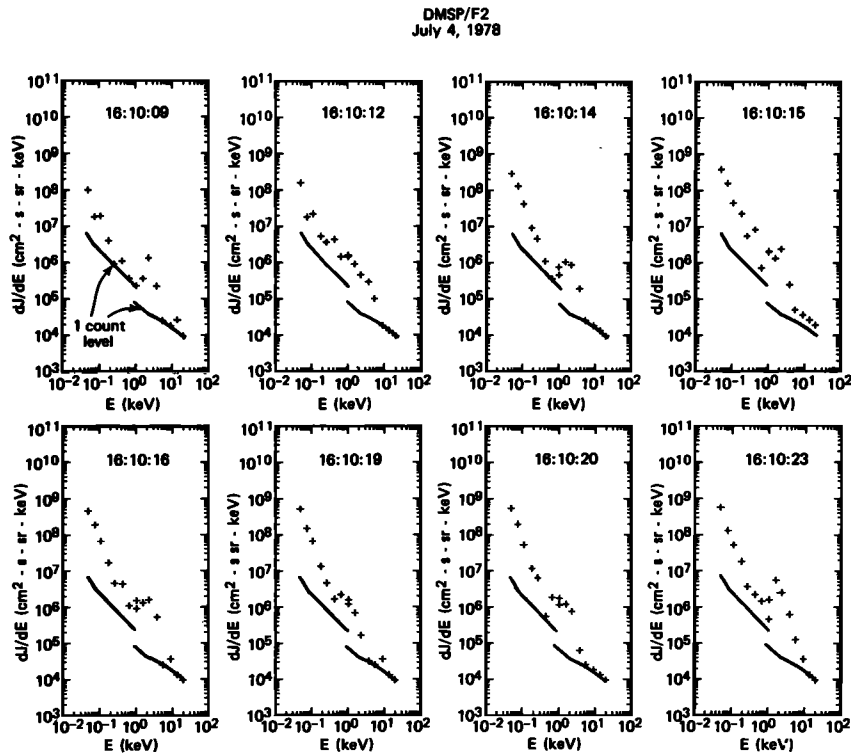


Fig. 6b. Electron spectra of precipitation equatorward of the diffuse aurora. Prominent secondary peaks are seen at 1–5 keV.



Fig. 8a. Another instance of 'ripples' on the equatorward boundary of the diffuse aurora at ~1148 UT on July 8, 1975, seen by DMSP/F1.

wave is nonzero. If the bending is due to wave steepening, then it implies that the wave propagates toward midnight. If the wave bending arises from a faster convection of the waveform at the high-latitude portion than at the low-latitude portion, then the wave propagation direction is toward afternoon.

The fact that the wave patterns occurring at the equatorward boundary of the diffuse aurora suggests that it may be a visual manifestation of a surface wave propagating on the inner edge of the plasma sheet. Their occurrence seems to be intimately related to the storm time ring current. It may be noted that from in situ observations [Frank, 1971], the outer

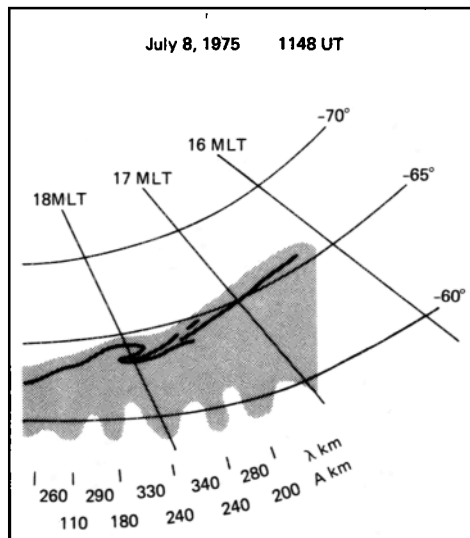


Fig. 8b. A schematic illustration of some auroral features in the southern polar region at ~1148 UT on July 8, 1975.

edge of the storm time ring current overlaps spatially with the inner edge of the plasma sheet in the evening-afternoon sector where the wave patterns reported here are seen. Hasegawa [1976] has suggested that energy in the disturbed magnetosphere is very likely converted to large-scale incompressible MHD perturbations mostly in the form of a surface wave. The inner edge of the plasma sheet and the outer edge of the ring current where sharp density gradients occur are possible locations. The observations here can be considered as consistent with his suggestion.

A fundamental question arising from these observations is what are the possible candidates for the plasma instability responsible for the observed undulations at the equatorward boundary of the diffuse aurora. Since there appears to be a large-scale configurational change of magnetospheric boundary associated with the observed phenomenon, microscopic instabilities, such as two stream instabilities, which do not produce configurational changes are obviously unlikely. One may consider the interchange instability as a possible candidate. However, the inner edge of the plasma sheet is stable against this instability because the magnetic field lines are curved into the plasma [e.g., Krall and

TABLE 2. American IMS Magnetic Stations Used

	C.G.	C.G.	June 26, 1978	July 4, 1978
	Latitude	Longitude		
Arctic Village	68.5°	258.4		X
Talkeetna	62.9	258.6	X	
College	64.4	260.5	X	X
Inuvik	70.7	268.7	X	X
Sach Harbour	76.2	269.7	X	X
Cape Perry	74.6	273.9		X
Fort Simpson	68.0	286.8	X	X
Pelly Bay	79.6	329.4	X	X

Trivelpiece, 1973]. This can simply be understood in terms of the analogy between the interchange instability and the Rayleigh-Taylor instability for a plasma supported against gravity by the magnetic field lines. In the interchange instability, the centrifugal force of plasma particles in bounce motions along the curved magnetic field lines plays the role of gravity. When magnetic field lines are curved into the plasma, it is analogous to gravity directed into the plasma and thus the system is stable. One may consider the interchange instability to act on the outer edge of the storm-time ring current [Chang *et al.*, 1965, 1966; Swift, 1967; Hasegawa, 1971a] and produce the observed wave pattern. However, it has been pointed out [Chang *et al.*, 1965, 1966; Hasegawa, 1971a] that a fractional amount of cold electrons can stabilize this instability. Electron measurements at low altitudes (Figure 6) and in the magnetosphere [e.g., Vasylunas, 1968] indicate that ample cold electrons are available at the equatorward boundary of the diffuse aurora and in the inner edge of the plasma sheet, suggesting that the interchange instability may not be the mechanism for the observed undulations. Drift wave instabilities have been discussed extensively with the ring current [Chamberlain, 1963; Liu, 1970; Hasegawa, 1971b,c], although there have been some attempts directed to explain auroral micropulsations [Coroniti and Kennel, 1970; Chance *et al.*, 1973]. Since the ring current appears to be stable

TABLE 1. List of DMSP Passes Showing Undulations at the Equatorward Boundary of the Diffuse Aurora

Date	Approximate Time	Figure References	Geomagnetic Conditions			Interplanetary Conditions						
			Kp	ΣKp	Dst	V_{SW}	n	Temperature	B	B_{λ}	B_{λ}	B_z
July 8, 1975	1148	8a,b	5	33+	-39	351	29.5	30	14.4	-2.2	5.7	-12.7
June 26, 1978	2043- 2240	1a,b	5	39	-69 -78	449 445	8.4 9.2	24 19				
		2a,b										
		3a,b										
July 4, 1978	1609	4a,b	8	43	-114							
Jan. 25, 1979	0406	9a,b	6-	34-	-45							

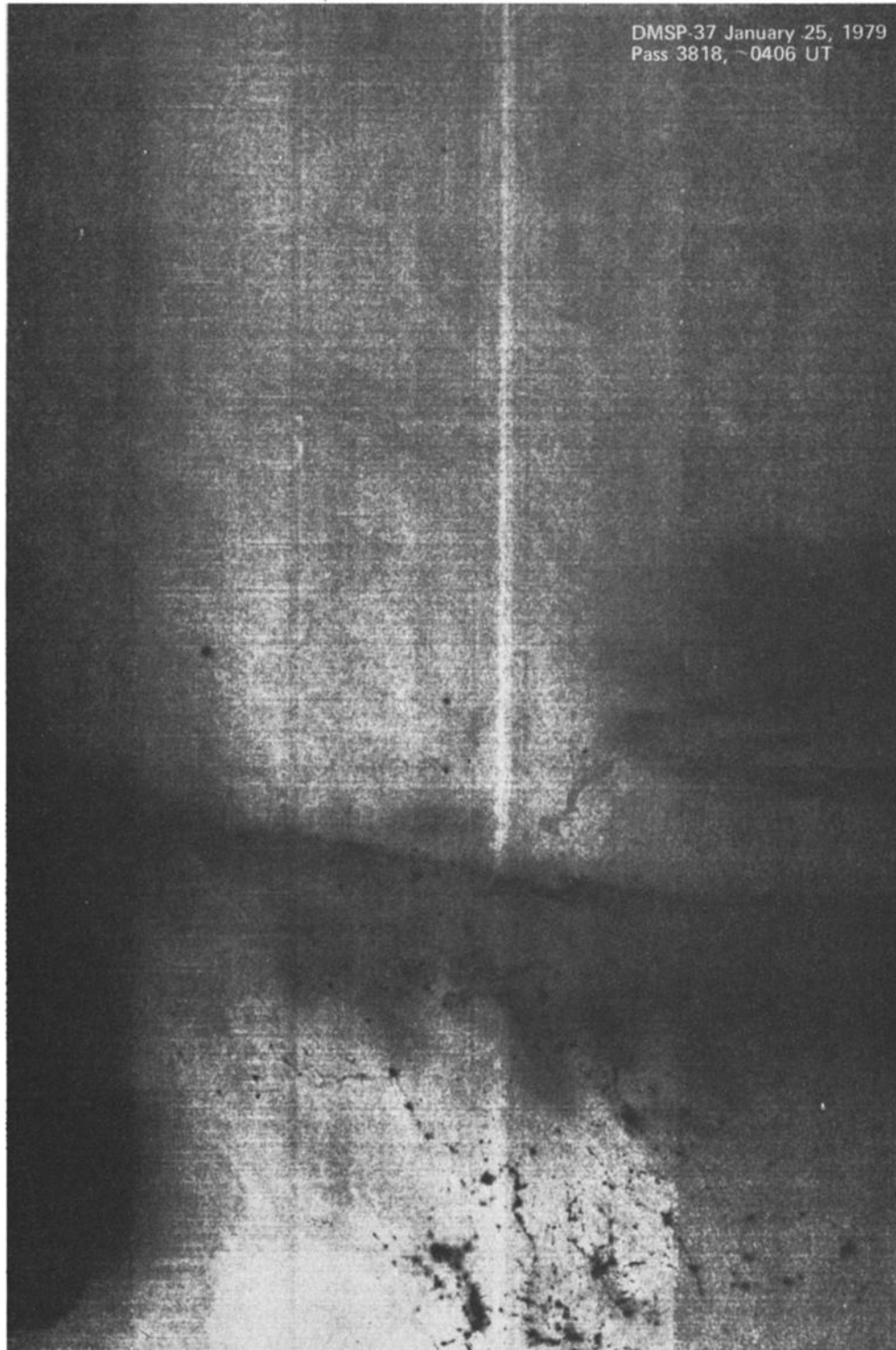


Fig. 9a. Irregular extrusions at the equatorward boundary of the diffuse aurora seen by DMSP/F3 at about 0406 UT on January 25, 1979.

against most of the drift mode instabilities [Hasegawa, 1971a], possibly the inner edge of the plasma sheet rather than the outer edge of the ring current may be susceptible to this type of instability. According to Hasegawa [1971a], these

instabilities usually have very small growth rates. This is not inconsistent with the observations here because comparison of the development of undulations in Figures 1b, 2b, and 3b suggests that the time scale for growth may be relatively long,

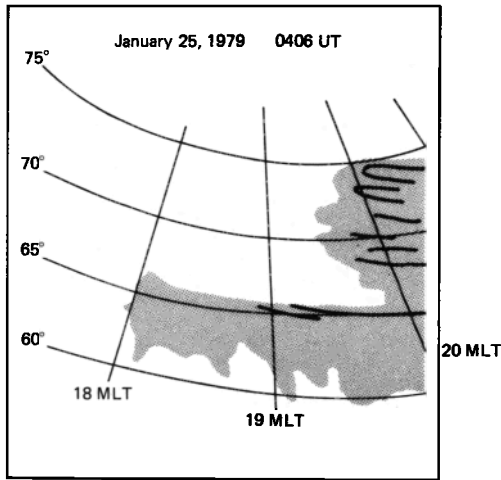


Fig. 9b. A sketch of the main auroral features in the northern polar region at about 0406 UT on January 25, 1979.

perhaps tens of minutes. Apart from drift wave instabilities, the Kelvin-Helmholtz instability is another possible candidate that can generate a surface wave. This instability is driven by the velocity shear across the boundary. It is possible that the velocity shear is set up by the sunward convection in the diffuse aurora (westward in the evening sector) and the corotation at the lower latitudes in the plasmasphere (eastward). It may be noted that this velocity shear is present even when there is no geomagnetic storm. Therefore, if the Kelvin-Helmholtz instability is the mechanism for the observed modulation, then it is necessary to explain why the inner edge of the plasma sheet appears to be stable against this instability at all times other than near the peak of a geomagnetic storm. This may perhaps be achieved by establishing an instability threshold that can be exceeded only during periods of geomagnetic storms.

Acknowledgments. We are indebted to S.-I. Akasofu, J. F. Carbary, and L. J. Zanetti for their constructive comments on the manuscript. We have also benefitted from discussion with R. L. Arnoldy, W. I. Axford, A. Hasegawa, R. L. Kaufmann, and C. F.

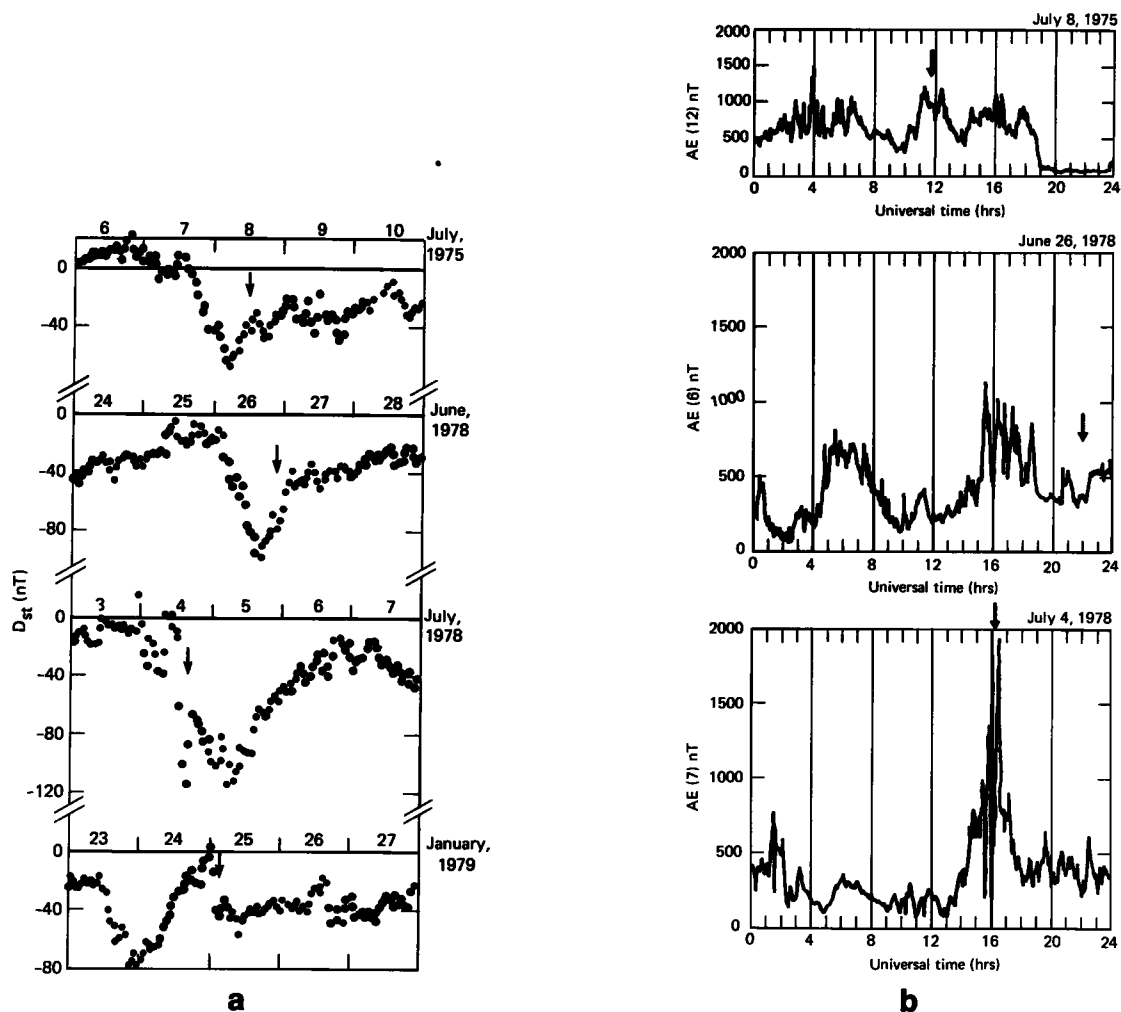


Fig. 10. (a) The D_{st} index for 5 days centered around the occurrence of undulation on the equatorward boundary of the diffuse aurora. (b) The AE index for the days on which undulation on the equatorward boundary of the diffuse aurora is seen in the afternoon-evening sector.

Kennel. This research is supported in part by the Air Force Office of Scientific Research under grant AFOSR-79-0010 and by the Division of Atmospheric Sciences, National Science Foundation under grants ATM-79-23240 and ATM-79-25987 to The Johns Hopkins University Applied Physics Laboratory.

The Editor thanks C. D. Anger and S. B. Mende for their assistance in evaluating this paper.

REFERENCES

- Akasofu, S.-I., A study of auroral displays photographed from the DMSP-2 satellite and from the Alaska meridian chain of stations, *Space Sci. Rev.*, **16**, 617, 1974a.
- Akasofu, S.-I. Discrete, continuous and diffuse auroras, *Planet. Space Sci.*, **22**, 1723, 1974b.
- Allen, J. H., C. C. Abston, J. E. Salazar, and J. A. McKinnon, Auroral electrojet magnetic activity indices AE(12) for July-December 1975, *Rep. UAG-76*, World Data Center A for Solar-Terrestrial Physics, Boulder, Colo., 1980.
- Anger, C. D., W. Sawchuk, and G. G. Shepherd, Polar cap optical aurora seen from ISIS 2, in *Magnetospheric Physics*, edited by B. M. McCormac, p. 357, D. Riedel Publ. Co., Boston, 1974.
- Anger, C. D., M. C. Moshupi, D. D. Wallis, J. S. Murphree, L. H. Brace, and G. G. Shepherd, Detached auroral arcs in the trough region, *J. Geophys. Res.*, **83**, 2683, 1978.
- Ashour-Abdalla, M., and R. M. Thorne, Toward a unified view of diffuse auroral precipitation, *J. Geophys. Res.*, **83**, 4755, 1978.
- Berkey, F. T., Temporal fluctuations in the luminosity of diffuse aurora, *J. Geophys. Res.*, **85**, 6075, 1980.
- Buchau, J., G. J. Gassmann, C. P. Pike, R. A. Wagner, and J. A. Whalen, Precipitation patterns in the arctic ionosphere determined from airborne observations, *Ann. Geophys.*, **28**, 443, 1972.
- Burke, W. J., D. A. Hardy, F. J. Rich, M. C. Kelley, M. Smiddy, B. Shuman, R. C. Sagalyn, R. P. Vancour, P. J. L. Widman, and S. T. Lai, Electrodynamical structure of the late evening sector of the auroral zone, *J. Geophys. Res.*, **85**, 1179, 1980.
- Chamberlain, J. W., Plasma instability as a mechanism for auroral bombardment, *J. Geophys. Res.*, **68**, 5667, 1963.
- Chance, M. S., F. V. Coroniti, and C. F. Kennel, Finite β drift Alfvén instability, *J. Geophys. Res.*, **78**, 7521, 1973.
- Chang, D. B., L. D. Pearlstein, and M. N. Rosenbluth, On the interchange instability of the Van Allen belt, *J. Geophys. Res.*, **70**, 3085, 1965.
- Chang, D. B., L. B. Pearlstein, and M. N. Rosenbluth, Corrections and additions to the paper entitled "On the interchange instability of the Van Allen belt," *J. Geophys. Res.*, **71**, 351, 1966.
- Coroniti, F. V., and C. F. Kennel, Auroral micropulsation instability, *J. Geophys. Res.*, **75**, 1863, 1970.
- Davis, T. N., O. Royovik, and T. J. Hallinan, Reply, *J. Geophys. Res.*, **83**, 5327, 1978.
- Eather, R. H., S. B. Mende, and R. J. R. Judge, Plasma injection at synchronous orbit and spatial and temporal auroral morphology, *J. Geophys. Res.*, **81**, 2805, 1976.
- Frank, L. A., Relationship of the plasma sheet, ring current, trapping boundary, and plasmopause near the magnetic equator and local midnight, *J. Geophys. Res.*, **76**, 2265, 1971.
- Gussenhoven, M. S., D. A. Hardy, and W. J. Burke, DMSP/F2 electron observations of equatorward auroral boundaries and their relationship to magnetospheric electric fields, *J. Geophys. Res.*, **86**, 768, 1981.
- Hardy, D. A., M. S. Gussenhoven, and A. Huber, The precipitating electron detectors (SSJ/3) for the Block 5D/Flights 2-5 DMSP satellites: Calibration and data presentation, *Rep. AFGL-TR-79-0210*, Air Force Geophys. Lab., Bedford, Mass., 1979.
- Hasegawa, A., Plasma instabilities in the magnetosphere, *Rev. Geophys. Space Phys.*, **9**, 703, 1971a.
- Hasegawa, A., Drift wave instability at the plasmopause, *J. Geophys. Res.*, **76**, 5361, 1971b.
- Hasegawa, A., Drift wave instability of a compressional mode in a high β plasma, *Phys. Rev. Lett.*, **27**, 11, 1971c.
- Hasegawa, A., Particle acceleration by MHD surface wave and formation of aurora, *J. Geophys. Res.*, **81**, 5083, 1976.
- Huber, A., J. Pantazis, A. L. Besse, and P. L. Rothwell, Calibration of the SSJ/3 sensor on the DMSP satellites, *Rep. AFGL-TR-76-0202*, AD-A045-977, Air Force Geophys. Lab., Bedford, Mass., 1977.
- Kamide, Y., and J. D. Winningham, A statistical study of 'instantaneous' nightside auroral oval. The equatorward boundary of electron precipitation as observed by ISIS 1 and 2 satellites, *J. Geophys. Res.*, **82**, 5573, 1977.
- King, J. H., Interplanetary medium data book-Appendix, NSSDC/WDC-A-R&S 77-04a, September, 1977.
- Krall, N. A., and A. W. Trivelpiece, Principles of plasma physics, McGraw-Hill, New York, 1973.
- Lincoln, J. V., Geomagnetic and solar data, *J. Geophys. Res.*, **80**, 4773, 1975.
- Lincoln, J. V. Geomagnetic and solar data, *J. Geophys. Res.*, **83**, 4882, 1978a.
- Lincoln, J. V., Geomagnetic and solar data, *J. Geophys. Res.*, **83**, 5329, 1978b.
- Liu, C. S., Low-frequency drift wave instabilities of the ring current belt, *J. Geophys. Res.*, **75**, 3789, 1970.
- Lui, A. T. Y., and C. D. Anger, A uniform belt of diffuse auroral emission seen by the ISIS 2 scanning photometer, *Planet. Space Sci.*, **21**, 799, 1973.
- Lui, A. T. Y., and J. R. Burrows, On the location of auroral arcs near substorm onsets, *J. Geophys. Res.*, **83**, 3342, 1978.
- Lui, A. T. Y., P. Perreault, S.-I. Akasofu, and C. D. Anger, The diffuse aurora, *Planet. Space Sci.*, **21**, 857, 1973.
- Lui, A. T. Y., C. D. Anger, and S.-I. Akasofu, The equatorward boundary of the diffuse aurora and auroral substorms as seen by the ISIS 2 scanning photometer, *J. Geophys. Res.*, **80**, 3603, 1975a.
- Lui, A. T. Y., C. D. Anger, D. Venkatesan, W. Sawchuk and S.-I. Akasofu, The topology of the auroral oval as seen by the ISIS 2 scanning auroral photometer, *J. Geophys. Res.*, **80**, 1795, 1975b.
- Lui, A. T. Y., D. Venkatesan, C. D. Anger, S.-I. Akasofu, W. J. Heikkila, J. D. Winningham, and J. R. Burrows, Simultaneous observations of particle precipitations and auroral emissions by the ISIS 2 satellite in the 19-24 MLT sector, *J. Geophys. Res.*, **82**, 2210, 1977.
- Meng, C.-I., B. Mauk, and C. E. McIlwain, Electron precipitation of evening diffuse aurora and its conjugate electron fluxes near the magnetospheric equator, *J. Geophys. Res.*, **84**, 2545, 1979.
- Moshupi, M. C., ISIS 2 observations of aurora in the ionospheric trough region, Ph.D. thesis, Univ. of Calgary, Calgary, Alta., 1977.
- Moshupi, M. C., L. L. Cogger, D. D. Wallis, J. S. Murphree, and C. D. Anger, Auroral patches in the vicinity of the plasmopause, *Geophys. Res. Lett.*, **4**, 37, 1977.
- Moshupi, M. C., C. D. Anger, J. S. Murphree, D. D. Wallis, J. H. Whitteker, and L. H. Brace, Characteristics of trough region auroral patches and detached arcs observed by ISIS 2, *J. Geophys. Res.*, **84**, 1333, 1979.
- Murphree, J. S., and C. D. Anger, Instantaneous auroral particle energy deposition as determined by optical emissions, *Geophys. Res. Lett.*, **5**, 551, 1978.
- Ossakow, S. L., and P. K. Chaturvedi, Current convective instability in the diffuse aurora, *Geophys. Res. Lett.*, **6**, 332, 1979.
- Pike, C. P., DAPP satellite observations of aurora, *EoS Trans. AGU*, **55**, 604, 1974.
- Pike, C. P., and E. H. Gardner, Looking down on the aurora from space, *Astronaut. Aeronaut.*, **19**, 64, 1981.
- Pike, C. P., and J. A. Whalen, Satellite observations of auroral substorms, *J. Geophys. Res.*, **79**, 985, 1974.
- Rogers, E. H., D. F. Nelson, and R. C. Savage, Auroral photography from a satellite, *Science*, **183**, 951, 1974.
- Royovik, O., and T. N. Davis, Pulsating aurora: Local and global morphology, *J. Geophys. Res.*, **82**, 4720, 1977.
- Sandford, B. P., Variations of auroral emissions with time, magnetic activity and solar cycle, *J. Atmos. Terr. Phys.*, **30**, 1921, 1968.
- Sheehan, R. E., and K. L. Carovillano, Characteristics of the equatorward auroral boundary near midnight determined from DMSP images, *J. Geophys. Res.*, **83**, 4749, 1978.
- Shepherd, G. G., F. W. Thirkettle, and C. D. Anger, Topside optical view of the dayside cleft aurora, *Planet. Space Sci.*, **24**, 937, 1976.
- Siren, J. C., Pulsating aurora in high latitude satellite photographs, *Geophys. Res. Lett.*, **2**, 557, 1975.
- Siren, J. C., Comment on 'Pulsating aurora: Local and global

- morphology' by O. Royovik and T. N. Davis, *J. Geophys. Res.*, **83**, 5325, 1978.
- Slater, D. W., L. L. Smith, and E. W. Kleckner, Correlated observations of the equatorward diffuse auroral boundary, *J. Geophys. Res.*, **85**, 531, 1980.
- Snyder, A. L., S.-I. Akasofu, and T. N. Davis, Auroral substorms observed from above the north polar region by a satellite, *J. Geophys. Res.*, **79**, 1393, 1974.
- Swift, D. W., The possible relationship between the auroral breakup and the interchange instability of the ring current, *Planet, Space Sci.*, **15**, 1225, 1967.
- Vasyliunas, V. M., A survey of low-energy electrons in the evening sector of the magnetosphere with Ogo 1 and Ogo 3, *J. Geophys. Res.*, **73**, 2839, 1968.
- Wallis, D. D., J. R. Burrows, M. C. Moshupi, C. D. Anger, and J. S. Murphree, Observations of particles precipitating into detached arcs and patches equatorward of the auroral oval, *J. Geophys. Res.*, **84**, 1347, 1979.
- Whalen, J. A., J. Buchau, and R. A. Wagner, Airborne ionospheric and optical measurements of noontime aurora, *J. Atmos. Terr. Phys.*, **33**, 661, 1971.
- Whalen, J. A., R. A. Wagner, and J. Buchau, A 12-hour case study of auroral phenomena in the midnight sector: Oval, polar cap, and continuous auroras, *J. Geophys. Res.*, **82**, 3529, 1977.
- Winningham, J. D., F. Yasuhara, S.-I. Akasofu, and W. J. Hedikkila, The latitudinal morphology of 10 eV to 10 keV electron fluxes during magnetically quiet and disturbed times in the 2100-0300 MLT sector, *J. Geophys. Res.*, **80**, 3148, 1975.

(Received June 5, 1981;
revised October 13, 1981;
accepted October 27, 1981.)